Journal of Cleaner Production 280 (2021) 124293

Contents lists available at ScienceDirect

Journal of Cleaner Production

journal homepage: www.elsevier.com/locate/jclepro

Compressive strength, modulus of elasticity and hardness of geopolymeric cement synthetized from non-calcined natural kaolin

Fernando Pelisser Prof., Dr. Eng. (Fernando) [a, *],
Adriano Michael Bernardin Prof., Dr. Eng. (Adriano) [b],
Milton Domingos Michel Prof., Dr. Eng. (Milton) [c],
Caroline Angulski da Luz Prof., Dr. Eng. (Caroline) [d]

[a] Civil Engineering Department, Federal University of Santa Catarina, 88040-900, Florianópolis, Santa Catarina, Brazil
[b] Graduation Program on Materials Science and Engineering, University of the Extreme South of Santa Catarina, 88806-000, Criciúma, Santa Catarina, Brazil
[c] Materials Engineering Department, State University of Ponta Grossa, 84030-900, Ponta Grossa, Paraná, Brazil
[d] Civil Engineering Department, Federal Technological University of Paraná, 85501-970, Pato Branco, Paraná, Brazil

ARTICLE INFO

Article history:
Received 11 April 2020
Received in revised form
24 August 2020
Accepted 16 September 2020
Available online 24 September 2020

Handling editor: Prof. Jiri Jaromir Klemeš

Keywords:
Geopolymeric cements
Natural kaolin
Sustainable materials
Green cements

ABSTRACT

In this work, a natural non-calcined kaolin was used for the synthesis of a geopolymeric paste. The effect of the natural kaolin characteristics and the alkaline activator ratio ($Na_2O.SiO_2/NaOH$) on the mechanical behavior of the resulting geopolymeric cement was determined. The chemical and mineral composition of the kaolin were determined by XRF and XRD techniques. For the synthesis, sodium silicate and sodium hydroxide were used in molar ratios of $Na_2O.SiO_2/NaOH = 1.0$, 1.6 and 2.2 and the curing of the samples was performed at 40 °C. The compressive strength of the samples was evaluated at 7 and 28 days of age. The modulus of elasticity and hardness were determined by instrumented nanoindentation. Microstructural analysis (SEM) combined with chemical analysis (EDS) was performed to study the morphology of the geopolymeric cement samples. The results showed that the natural kaolin is 95% amorphous (Rietveld) and shows small particle size (<5 μm, by SEM). The most efficient composition, with $Na_2O.SiO_2/NaOH = 2.2$ ratio, showed a modulus of elasticity of 10 GPa, hardness of 0.4 GPa and compressive strength of 67 MPa. In the microstructural analysis, the surface of the samples showed some cracks, probably caused by the curing process, and small roughness, but the cured specimens did not show visible flaws. The high strength is due to the chemical composition of the cement, with a SiO_2/Al_2O_3 ratio of 3.5, and due to the degree of amorphism of the natural kaolin, 95%. Therefore, the use of a natural kaolin, without further calcination, reduces costs and environmental impacts in the design of geopolymeric cements.

1. Introduction

The growing demand for concretes showing high-efficiency, low-cost and low environmental impact, especially when compared to ordinary Portland cement (OPC) concretes, has promoted the development of clinker-free cementitious materials, including geopolymeric cements (Tan et al., 2020; Assi et al., 2020).

Geopolymers are also known as alkali-activated materials, whose use may contribute to the reduction of carbon footprint in the building industry (Provis, 2013; Shia et al., 2019; Singh and Middendorf, 2020). The study of alkali-activated cements (AACs) is growing fast in the global research community (Provis et al., 2015; Gartner and Sui, 2018).

The study of AACs can be considered as a challenging research area with economic and environmental impacts. These cements can be produced using a wide variety of raw materials (Provis et al., 2015; Firdous et al., 2018; Shia et al., 2019), and industrial waste (Longhi et al., 2016; Tan et al., 2020; Assi et al., 2020), as they do not require materials with a high degree of purity and uniformity. The

* Corresponding author.
E-mail addresses: f.pelisser@ufsc.br (F. Pelisser), amb@unesc.net (A.M. Bernardin), mdmichel@uepg.br (M.D. Michel), angulski@utfpr.edu.br (C.A. da Luz).

https://doi.org/10.1016/j.jclepro.2020.124293
0959-6526/

AACs show low cost of energy consumption and low emission of carbon dioxide (CO_2). AACs produced from fly ash, blast furnace slag and natural pozzolans can reach up to 80% reduction of CO_2 emissions in comparison to Portland cement (Van Deventer, Provis and Duxson, 2012; Bajpai et al., 2020; Amran et al., 2020).

In this way, the use of geopolymers in construction projects can contribute to the reduction of CO_2 emissions (carbon footprint). As stated, geopolymeric cements generally show lower CO_2 emissions – when compared to ordinary Portland cements – due to two main reasons. First, industrial residues can be used as raw materials, giving an adequate destination to them. And the standard metakaolin used for the synthesis of geopolymers is calcined at much lower temperatures (700 °C) than Portland cement (1450 °C). Second, there is much less emission of CO_2 when preparing the geopolymeric cement in comparison with the decarbonation of limestone during the production of clinker for the manufacturing of Portland cement, thus resulting in lower CO_2 emissions and energy expenditure in the process. Some works show that the energy spent to produce one ton of metakaolin is approximately 2.95 GJ, against approximately 4.7 GJ for Portland cement. Approximately 175 kg of CO_2 is emitted into the atmosphere due to the production of metakaolin (Cassagnabère et al., 2010; Bajpai et al., 2020; Amran et al., 2020) in comparison to what is emitted for clinker production (800 kg of CO_2/ton).

Although the work of Turner and Collins (2013), considering all manufacturing and application processes, do not show this advantage, such differences depend on several factors, ranging from the quality and costs of the starting materials in some places, until the composition, production and performance of the obtained geopolymeric concretes (Medri et al., 2020; Ng et al., 2018). However, some studies show the economic viability to produce geopolymeric cements, reaching values of approximately US$ 150 per cubic meter (Ozel, 2012; Shia et al., 2019; Gartner and Sui, 2018), even considering the current restricted demand. Despite the excellent performance of Portland cement in the production of concretes and mortars, the geopolymeric cements show competitive mechanical properties and satisfactory durability (Ng et al., 2018; Firdous et al., 2018; Singh and Middendorf, 2020).

Geopolymers are a three-dimensional network of aluminosilicates, amorphous in nature and with a semicrystalline structure. Their empirical formula can be described by: $M_n[-(SiO_2)_z-AlO_2]_n.-wH_2O$, where z is 1, 2 or 3, M is an alkali metal cation, an n is the degree of polycondensation (Davidovits, 1991; Gartner and Sui, 2018). The complex structure of the geopolymeric system consists of chains, sheets and three-dimensional networks formed by several types of Q units of connected SiO_4 and AlO_4 tetrahedra. As a source of aluminosilicates, many types of calcined clays can be used for cement production, among which, metakaolin is frequently used (Medri et al., 2020).

Even if the chemical composition of the raw materials used in the synthesis is an important factor in the performance of the geopolymeric cement, Reddy et al. (2016) showed, through a data search, that the best results of compressive strength were found for a chemical composition varying from 45 to 55% of SiO_2, 22–28% of Al_2O_3 and 15–20% of Na_2O. The authors also showed that, even considering the best performance range, there is a very large difference of the obtained results, as an example, for the compressive strength, with a range of 20–60 MPa for very similar chemical compositions. Indeed, this effect is due to the reactivity of the starting materials, that relies on the processing techniques and on the characteristics of the clay minerals used as raw materials (Ma et al., 2018; Medri et al., 2020; Zhang et al., 2020).

Therefore, this work aimed at evaluating the potential use of a natural kaolin, originally used by the ceramic industry, without calcination, to produce geopolymeric cements. The study evaluated the mechanical properties of the produced cements, considering the effect of the alkaline activator ratio ($Na_2O.SiO_2$/NaOH).

The novelty of the work is the use of a natural kaolin for the synthesis of a geopolymeric composition. Usually, for the synthesis of geopolymers, calcined kaolin is used to obtain metakaolin (MK). MK is used because it is a metastable, non-crystalline and reactive mineral phase. However, is this work, a natural occurring, non-crystalline (95% amorphous) and fine (<5 μm particle size, by SEM image) kaolin was used instead of a calcined MK for the synthesis of a geopolymeric composition. The mechanical behavior of the composition was determined by compressive strength tests and by nanoindentation tests.

2. Materials and methods

The materials used for the composition of the geopolymeric cements were: a) natural kaolin, supplied by Esmalglass do Brasil company; b) sodium silicate, from Sigma-Aldrich (SiO_2 = 26.5%, Na_2O = 10.6%, and H_2O = 63.0%); and c) sodium hydroxide, from F Maia company (NaOH = 97%). The concentrations of the alkaline activator were determined, by molar ratio, as 2.2 for K1 composition, 1.6 for K2 composition and 1.0 for K3 composition (Table 1).

To prepare the mixtures (K1, K2 and K3) of the geopolymeric cements, the following procedure was adopted: i) pellets of sodium hydroxide (97%) were added into the sodium silicate solution in molar ratios given in Table 1, and the solutions were mixed in a magnetic stirrer; ii) kaolin was added to the alkaline solutions using a mechanical mixer; the mixing was performed for 4 min; iii) the mixtures were cast into cylindrical molds (2 cm height and 4 cm diameter) and the temperature of curing (setting) was fixed at 40 °C. The mixing procedure and a detail of a sample after demolding is shown in Fig. 1.

Table 1 shows the composition of the geopolymeric cements according to the SiO_2/Na_2O, SiO_2/Al_2O_3, Na_2O/Al_2O_3 and $Na_2O.SiO_2$/NaOH ratios. The water/kaolin ratio was fixed at H_2O/kaolin = 0.75 for each composition, according to the original amount of water in the sodium silicate solution. The $Na_2O.SiO_2$/NaOH ratio was ranged considering previous mechanical results with better performance (Pelisser et al., 2013), and references in the literature of existing relationships to obtain better polymerization (Davidovits, 1991; Cassagnabère et al., 2010; Heah et al., 2012).

The compressive strength was determined according to the ASTM C 1231(2010) standard and the specimens were tested at 7 and 28 days of age using 3 replicates for each sample. A universal testing machine (EMIC DL 10000, Brazil) was used with a loading rate of 0.5 MPa/s.

For the nanomechanical tests, an XP nanoindentator (MTS System, USA) was used. The modulus of elasticity (E) and hardness (H) were determined using a Berkovich tip.

The procedure for the nanoindentation technique is the controlled penetration of a diamond tip into the surface of the material and the recording of the charge and depth of penetration, at a nanoscale. The maximum load is held constant for a few seconds and then removed. The time, in seconds, is controlled in three stages: on loading, on full load and on unloading. The data is shown

Table 1
Composition, by molar ratio, of the geopolymeric cements.

Composition	K1	K2	K3
SiO_2/Na_2O	6.41	6.41	6.41
SiO_2/Al_2O_3	3.47	3.47	3.47
Na_2O/Al_2O_3	0.54	0.54	0.54
$Na_2O.SiO_2$/NaOH	2.20	1.60	1.00
H_2O/kaolin (g/g)	0.75	0.75	0.75

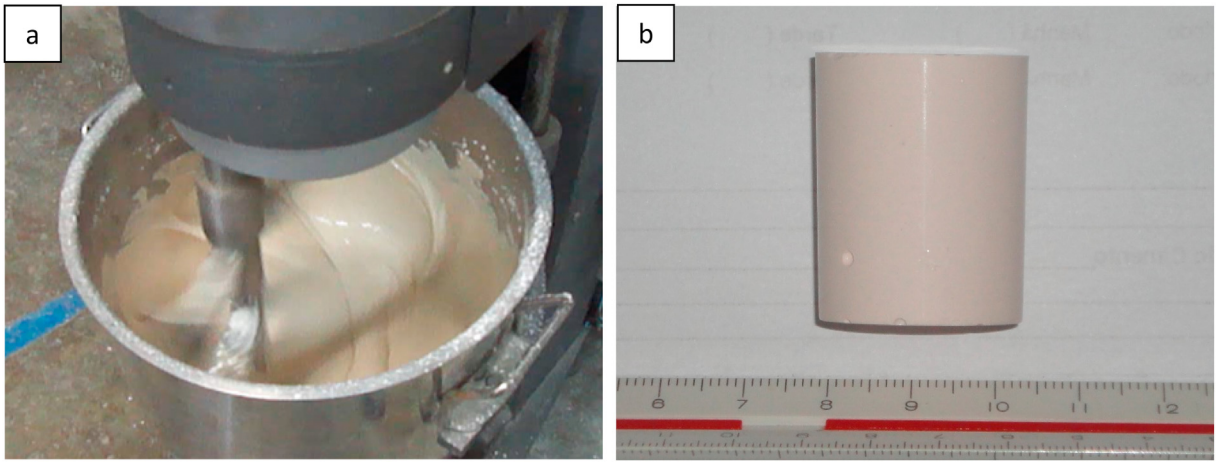

Fig. 1. (a) Mixing procedure for the preparation of the geopolymeric samples; (b) detail of a geopolymeric sample after demolding.

as a, which describes the charge-discharge characteristic of the material.

The modulus of elasticity (E) and the hardness (H) were determined from the load-displacement diagrams (P-h) for each sample, according to equations (1) and (2) (Oliver and Pharr, 1992, 2004). The hardness (H) of the samples were determined by:

$$H = \frac{P_{máx}}{A(h_c)} \quad (1)$$

where P_{max} is the maximum load and $A(h_c)$ is the projected contact area considering the effect of the Berkovich tip.

The modulus of elasticity (E) of the samples was determined by (Brotzen, 1994):

$$E = \frac{1-\nu^2}{\left(\frac{1}{E_r} - \frac{1-\nu^2}{E_i}\right)} \quad (2)$$

where, E_r is the reduced modulus of elasticity, E_i and ν are the modulus of elasticity and Poisson ratio of the indenter, and E and ν are the modulus of elasticity and Poisson ratio of the sample, respectively. For a diamond tip, $E_i = 1141$ GPa and $\nu_i = 0.07$ (Oliver and Pharr, 1992, 2004).

And the reduced modulus of elasticity (E_r) can be determined by (Sneddon, 1965; Oliver and Pharr, 1992, 2004):

$$E_r = \frac{\sqrt{\pi}}{2\beta}\frac{S}{\sqrt{A(h_c)}} \quad (3)$$

where $S = (dP/dh)$ is the stiffness of the sample determined from the upper part of the unloading curve, and β is a constant, dependent on the indenter geometry, equal to 1.034 for a triangular symmetry (Oliver and Pharr, 1992; Brotzen, 1994).

For the nanomechanical tests, samples with 5 mm thickness were prepared using a low speed cutter (Buehler Isomet). The samples surface was grinded using silicon carbide sandpaper (800 and 1200 grits). In sequence, polishing was performed using diamond paste (6, 1 and 0.25 μm particle sizes) to obtain the surface finish. The samples were polished for 30 min in each diamond paste size. After grinding/polishing, the samples were cleaned in an ultrasonic bath (15 min) to remove the dust and diamond particles from the surface and pores. After preparation, the samples were stored in a vacuum desiccator until testing. Sixteen indentations were made on the finished surface (testing area) in a pattern of 4×4 points (distancing 50 μm from each other) under 2, 4, 8, 16, and 32 mN loading cycles. The loading cycle was applied for 10 s, the maximum load was kept for 5 s and the unloading was performed in 10 s.

Scanning electron microscopy and elemental microanalysis (SEM/EDS) (Shimadzu SSX-550, Japan) was performed on the indented regions to determine differences in morphology and in chemical composition. The tests were performed on polished samples of 1 cm in diameter and 5–6 mm thickness.

Chemical analysis was performed using the X-ray fluorescence technique in a S2 Ranger (Bruker, USA) analyzer on molten samples. Crystallographic analysis was performed by X-ray diffraction in a D2 Phaser (Bruker, USA) using powdered samples (2θ from 10 to 80°, 2°/min scanning rate, 30 kV and 30 mA acceleration voltage and $CuK_{\alpha 1}$ incident radiation with $\lambda = 1{,}5406$ Å).

3. Results and discussion

The chemical analysis of the natural kaolin is shown in Table 2. The kaolin shows a SiO_2/Al_2O_3 ratio of 1.19. Comparing to a pure kaolinite sample ($Al_2O_3.2SiO_2.2H_2O$) that shows as stoichiometric composition 39.5% Al_2O_3, 46.5% SiO_2 and 14% H_2O, the sample of kaolin used in this study is very pure, with low contamination. Ng et al. (2018), in their review about pastes, mortars and concrete geopolymers, comment on the chemical composition of natural raw materials used to produce geopolymeric cements. The chemical composition of the natural kaolin from this work is similar to that of kaolin and calcined kaolin from the review. Silica an alumina are the main oxides and the loss on ignition is due to the dihydroxylation. The chemical composition is also similar to some source materials described by Assi et al. (2020).

The X-ray diffractometry of the natural kaolin is shown in Fig. 2. In the XRD spectrum, an amorphous halo can be observed between 15 and 35°, characterizing the disordered nature of the sample (Fig. 2). A peak at 27.5° is observed, ascribed to quartz (PDF file

Table 2
Chemical composition of the natural kaolin (XRF).

Oxide	mass (%)
SiO_2	46.7
Al_2O_3	39.1
Fe_2O_3	0.34
K_2O	0.36
Loss on ignition	13.4

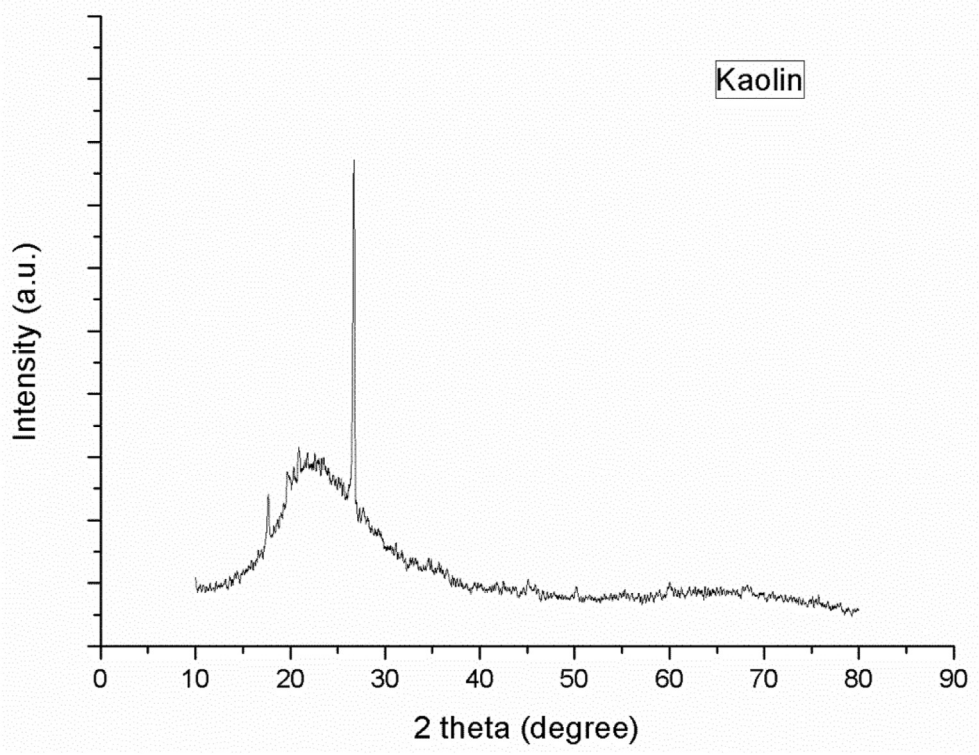

Fig. 2. XRD spectrum of the natural kaolin.

number 00-046-1045), the only contamination of the sample. The degree of amorphism of the kaolin sample is 95%, determined by the Rietveld method.

The microstructure of the kaolin sample (SEM) by secondary electron (SE) image is shown in Fig. 3a. The particles are granular and range from 1 to 5 μm. The backscattered electron (BSE) image is shown in Fig. 3b. Therefore, by the XRF, XRD and SEM analyzes, the sample of kaolin used in this study is pure, with no contamination besides quartz, is amorphous in nature and shows a granular texture.

The reaction mechanism when kaolin is added to the alkaline solution is the alkaline activation of an aluminosilicate material. When a solid with adequate ratio of reactive silicate and aluminate is mixed with a liquid with a high alkali concentration the geopolymerization process takes place. The polymerization process is like the reactions that result in the formation of zeolites. Initially, the Al and Si from the aluminosilicate are dissolved by the alkaline solution and react to form complex hydroxyaluminosilicates. The end product is the geopolymer, an alkaline aluminosilicate hydrate ($Na_2O \cdot Al_2O_3 \cdot 2SiO_2 \cdot nH_2O$) with a three-dimensional structure that resembles zeolites on an atomic to nanometric scale (Davidovits, 1991; 2012; Firdous et al., 2018; Medri et al., 2020).

The compressive strength of the geopolymeric compositions in function of the concentrations of the activator, at the ages of 7 and 28 days, is shown in Fig. 4. The best result, 67 MPa, was obtained for the composition K1 at 7 days of age, corresponding to the molar ratio $Na_2O.SiO_2/NaOH = 2.2$. The compressive strength for the composition K2 ($Na_2O.SiO_2/NaOH = 1.6$), 65 MPa, was close to K1. For the composition K3, with lower concentration of the alkaline activator (1.0), a small reduction was observed (60 MPa). Firdous et al. (2018) reviewed the use of natural pozzolans, mainly volcanic ones, to produce geopolymeric systems. They stated that the

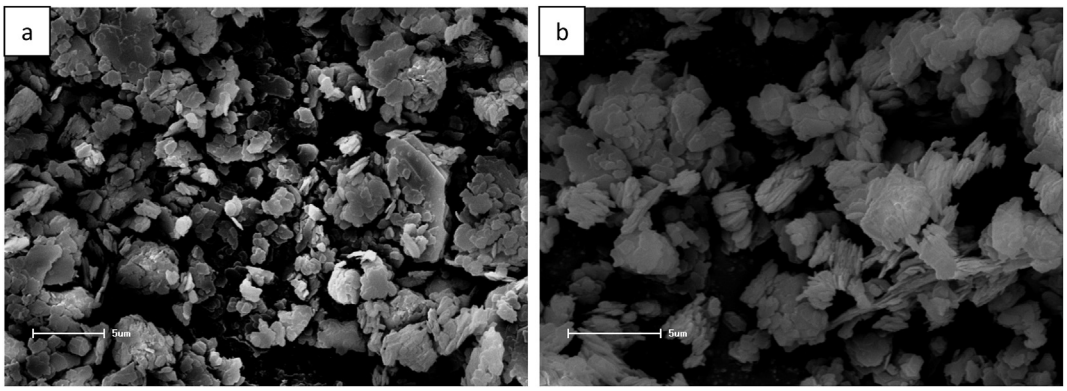

Fig. 3. Microstructure of the kaolin sample (SEM): (a) SE image; (b) BSE image.

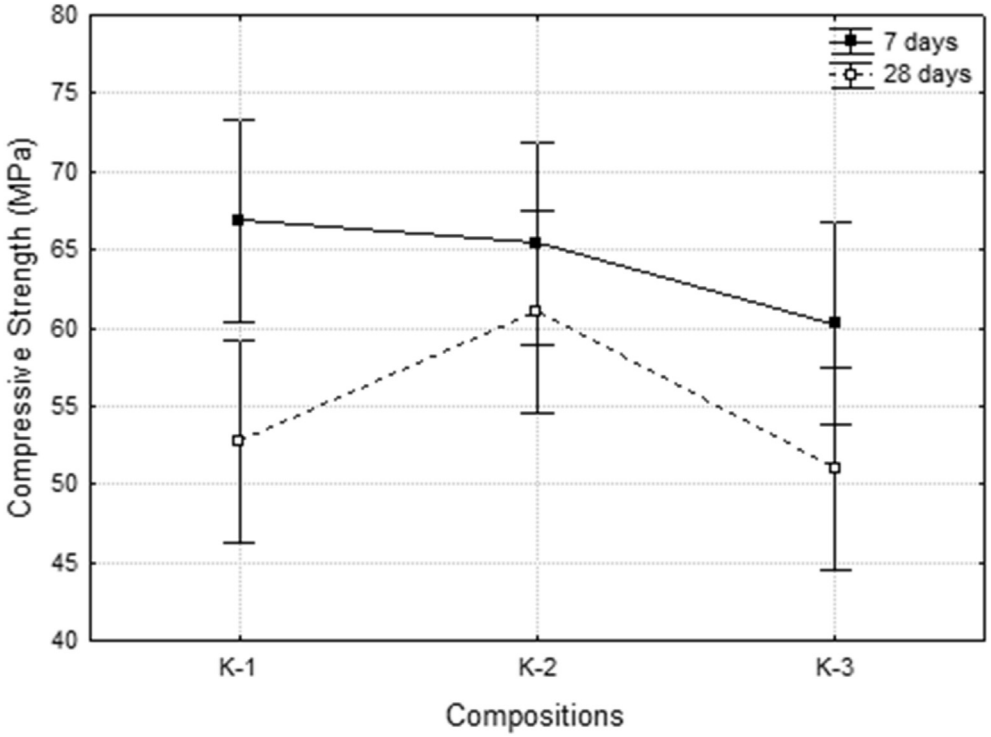

Fig. 4. Compressive strength of the geopolymeric compositions K1, K2 and K3 at the ages of 7 and 28 days.

main factors affecting the degree of geopolymerization are particle size, type and concentration of alkali activator, pre-treatment of raw material and curing conditions. For NaOH solutions, the compressive strength ranged from 27 to 43 MPa for concentrations ranging from 2.5 to 10 M. The samples were cured at 40 and 60 °C and autoclaved.

These results are in accordance with the trend that higher compressive strength is obtained when the $Na_2O.SiO_2$/NaOH ratio is increased (Heah et al., 2012). A similar behavior is shown for a geopolymeric cement based on fly ash (Chindaprasirt et al., 2006), in which the optimum $Na_2O.SiO_2$/NaOH ratio for the maximum strength was found between 0.67 and 1.0. It must be stated that the geopolymeric cement based on natural kaolin, in this work, shows high compressive strength due to the amorphous nature of the material. The disordered structure of the starting material and the chemical composition of the mixtures can be considered the most important factors for the design of a geopolymeric cement.

In this work, the mechanical behavior of the geopolymeric cements synthetized with natural kaolin, determined by the nano-indentation method, was similar to that of Pelisser et al. (2013) for geopolymers produced with metakaolin, reaching a compressive strength of 65 MPa. Geopolymeric cements showing compressive strengths above 65 MPa are not usual. Longhi et al. (2016) reported geopolymeric compositions reaching 72 MPa of compressive strength for a SiO_2/Al_2O_3 molar ratio of 3.5, however, at 50 °C curing temperature, in comparison to 40 °C used in this work.

Considering the $Na_2O.SiO_2$/NaOH ratio shown in Table 2 and the results of compressive strength shown in Fig. 4, the increase in this ratio improved the compressive strength, and the maximum strength was given for the intermediate ratio (K2 = 1.6), but the results for K1 and K2 are very similar. According to the literature, if the concentration of the alkaline activator increases, the polymerization is more complete (Rashad, 2013; Reddy et al., 2016; Singh and Middendorf, 2020). But if there is an excess, it is impaired, which is the case for the K3 ratio (= 2.2). This was the aim of the work, to verify the variation of the $Na_2O.SiO_2$/NaOH ratio on the strength of the geopolymeric cement, being therefore used the three concentrations of NaOH.

In a recent study, Reddy et al. (2016) have investigated the effect of the chemical composition on the mechanical performance of geopolymeric concretes. The chemical composition has a significant influence on the compressive strength. For example, SiO_2, Al_2O_3 and CaO should be in the ranges of 45–55%, 22–28%, 15–20%, respectively, for the best results. However, small variations in composition may exhibit large variations in strength. Although the chemical composition points out the performance of the cement, the reactivity of the raw materials – given by the amorphous or crystalline nature of them – may explain those differences in strength. The geopolymeric compositions of this work are in the range studied by Reddy et al. (2016), considering the chemical composition of the raw materials and the geopolymeric cements (Table 3). Also, Davidovits (1991) and Rashad (2013) stated that a SiO_2/Al_2O_3 molar ratio near 3 is optimal for the geopolymerization process. In this work, the SiO_2/Al_2O_3 ratio is 3.0.

These results show that the XRD analysis, used to determine the amorphousness of the starting material, is an important quantitative result for the use of different clay-minerals and industrial wastes for the formulation of efficient geopolymeric cements.

In order to characterize the micro-nanomechanical behavior of

Table 3
Chemical analysis for compositions K1, K2 and K3, determined by EDS technique.

Elements	Compositions (mass %) [a]		
	K1	K2	K3
Si	44.6	30.5	42.6
Al	20.6	14.6	21.2
O	23.1	19.6	22.6
Na	11.8	10.2	13.5

[a] The Au element, from the sample preparation, was not considered.

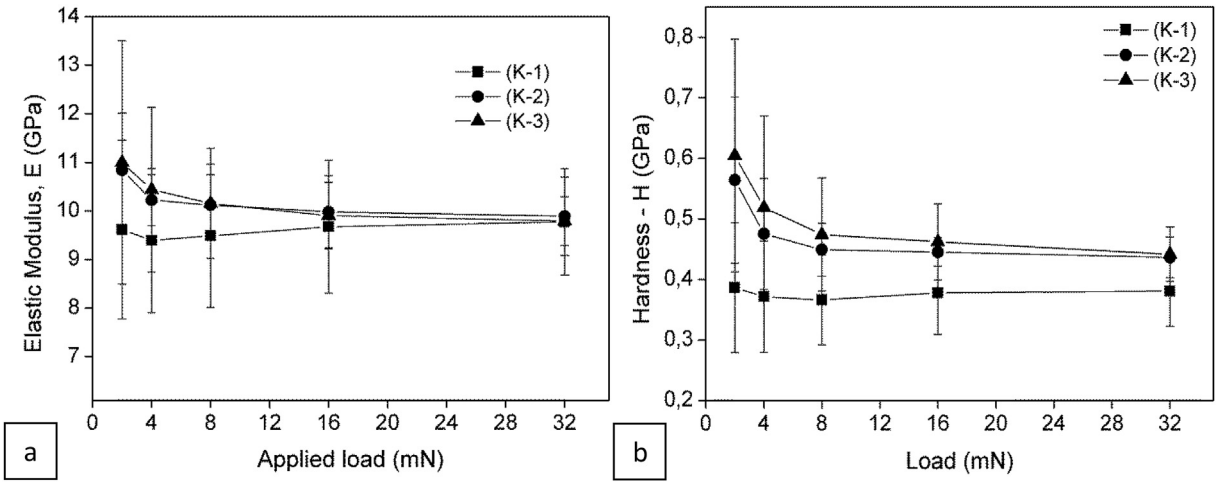

Fig. 5. (a) Modulus of elasticity and (b) hardness for the geopolymeric compositions K1, K2 and K3 in function of loading.

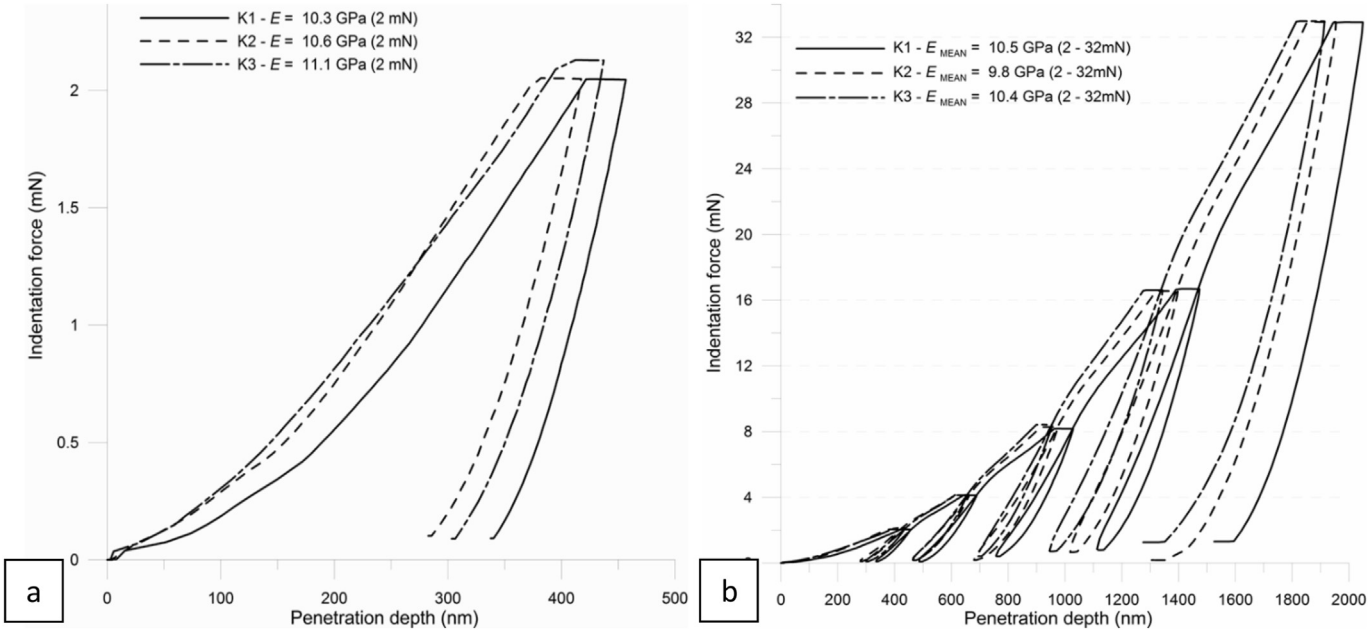

Fig. 6. Load-displacement curve for: (a) 2 mN loading; and (b) 2–32 mN loading, by nanoindentation, for cements with different $Na_2O.SiO_2$/NaOH ratios.

the geopolymeric cements, the modulus of elasticity and hardness of the geopolymers were studied. The average results for the modulus of elasticity and for hardness are shown in Fig. 5 for the compositions K1, K2 and K3.

The nanomechanical properties of the three geopolymeric cements were determined by 12 indentations. The modulus of elasticity for all compositions ranged from 9.7 to 11 GPa for small loading (2 mN) until 10 GPa for higher loading (32 mN), Fig. 5a. Regarding hardness, Fig. 5b, the variation was higher, ranging from 0.4 GPa for composition K1 (2–32 mN range) to 0.6 GPa for composition K3 at 2 mN loading. At higher loading (32 mN) the differences are small.

The displacement-load curves for all geopolymeric compositions is shown in Fig. 6 for 2 mN loading and for the 2–32 mN range. Differences in the modulus of elasticity are small and not significant for small loading (2 mN) (Fig. 6a), as observed by the modulus of elasticity (Fig. 5a) curve. Differences are higher for higher loadings (8–32 mN), Fig. 6b, but are not significant.

The statistical analysis (ANOVA, 95% reliability) shows a non-significant effect of the load used (2–32 mN). However, the reduction of the modulus of elasticity with increasing load can be explained by the occurrence of microcracks during the loading and unloading cycles. It must be noted that the modulus of elasticity was measured during the unloading cycle, and the results were recorded only in the elastic regime of the material.

The average and standard deviation for all 12 indentations performed on the geopolymeric cement with $Na_2O.SiO_2$/NaOH = 1.6 is shown in Table 4 for composition K2 in the load range of 2–32 mN.

SEM images of the surface where the indentation was performed for the composition K2 is show in Fig. 7. The surface is even and presents small roughness. An image of the nanoindentation matrix with 12 indentations is shown in Fig. 7a and the magnification (4500×) of the indentation area is shown in Fig. 7b. The micrographs show the homogeneity of the surface, resulting in the reliability of the measurements.

Table 4
Modulus of elasticity (E, GPa) and hardness (H, GPa) for the 12 indentations performed on composition K2 ($Na_2O.SiO_2$/NaOH = 1.6) in the load range of 2–32 mN. The data show the average and standard deviation for each indentation.

Indentation	Load (mN)											
	2		4		8		16		32		Average	
	E	H	E	H	E	H	E	H	E	H	E	H
1	8.6	0.49	8.2	0.31	9.7	0.31	9.7	0.31	10.4	0.32	9.3	0.35
2	8.0	0.29	7.6	0.26	8.2	0.27	7.9	0.28	8.4	0.26	8.0	0.27
3	12.2	0.60	9.9	0.49	9.2	0.37	8.3	0.33	8.2	0.27	9.6	0.41
4	8.7	0.37	8.0	0.28	9.0	0.25	9.1	0.27	9.9	0.28	8.9	0.29
5	10.1	0.24	9.7	0.28	9.1	0.31	8.7	0.28	8.9	0.28	9.3	0.28
6	10.5	0.41	10.2	0.35	10.8	0.34	10.8	0.37	10.3	0.37	10.5	0.37
7	12.4	0.46	13.1	0.50	12.5	0.53	11.3	0.53	10.7	0.48	12.0	0.50
8	10.3	0.40	9.3	0.39	8.9	0.37	9.1	0.37	9.2	0.27	9.4	0.36
9	9.4	0.38	9.5	0.28	9.9	0.28	11.5	0.30	11.5	0.36	10.4	0.32
10	12.5	0.38	13.0	0.42	12.6	0.46	12.2	0.48	11.7	0.47	12.4	0.44
11	9.1	0.29	9.4	0.30	10.4	0.33	10.8	0.38	11.0	0.42	10.1	0.34
Average	10.2	0.39	9.8	0.35	10.0	0.35	10.0	0.35	10.0	0.34	10.2	0.39
S.D.	1.6	0.10	1.8	0.09	1.4	0.08	1.4	0.08	1.2	0.08	1.6	0.10

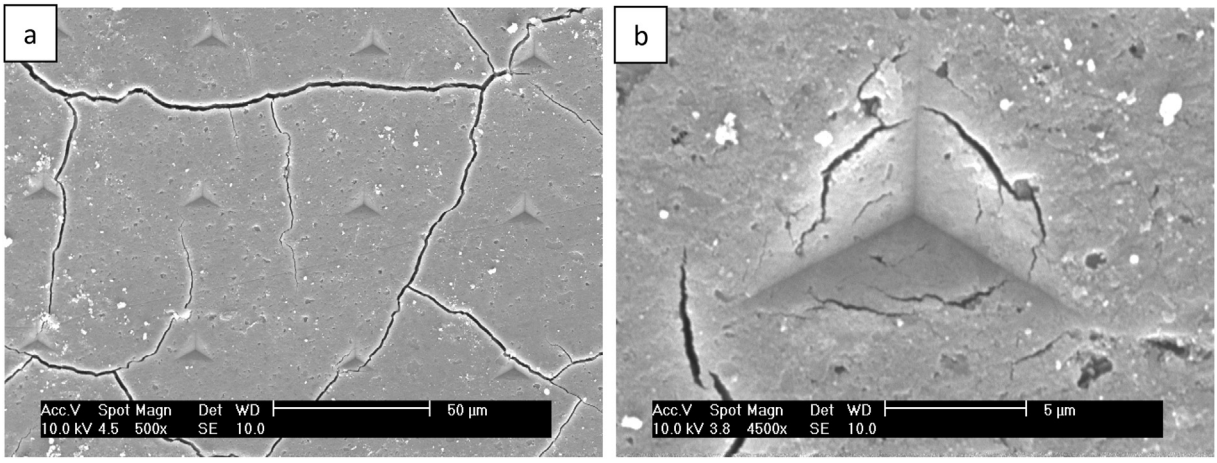

Fig. 7. SEM images of the surface of composition K2, $Na_2O.SiO_2$/NaOH = 1.6: (a) image of the nanoindentation matrix with 12 indentations; (b) detail of one indentation.

The surfaces of compositions K1 and K3 are shown in the SEM images of Fig. 8. There are no significant differences in morphology among all samples. The surfaces are even, with some cracks probably caused by the setting process and show small roughness.

A study on geopolymeric cements based on metakaolin and fly ash, activated with sodium silicate, showed results of modulus of elasticity – determined by nanoindentation – between 17 and 18 GPa (Nemecek et al., 2011). A load of 2 mN was used and a penetration-displacement of 300 nm was observed on the surface of the sample. The micro-nanomechanical results for a cement based on metakaolin were also close to the results observed in this work (Pelisser et al., 2013).

In this work, the results for modulus of elasticity (approximately 10 GPa) and for hardness (approximately 0.4 GPa) for the geopolymeric cements produced with natural kaolin are close to the results for hydrated Portland cement and for hydrated calcium silicate (C–S–H).

For Portland cement, the results were 10–15 GPa for the modulus of elasticity and 0.2–1.0 GPa for hardness, using loads ranging from 2 to 32 mN (Pelisser et al., 2011). For synthetic C–S–H with Ca/Si ratio = 2.1, the results were 15–20 GPa for the elastic modulus and 0.2–0.4 GPa for hardness (Pelisser et al., 2012).

Similar results were shown by Nemecek et al. (2011), when comparing the modulus of elasticity, determined by nanomechanical tests, of alkali-activated cements and C–S–H cements. The similarity between the mechanical behavior of both types of cement – alkali-activated and C–S–H – enables the development of hybrid cements, a more efficient form of cement, as already pointed out by Palomo et al. (2007). In general, the nanomechanical results are closer for hardness – for both cements – than for the modulus of elasticity, which shows a tendency to be lower, therefore typical of a more deformable material.

Regarding the use of kaolin as aluminosilicate precursor, Longhi et al. (2016) have studied the use of kaolin tailings for the synthesis of geopolymeric cements. The waste was formed mainly by kaolinite (~92%) contaminated with quartz and anatase. The resulting geopolymer had a compressive strength of 72 MPa at 28 days of age, that reduced to 62 MPa at 90 days of age for a silica/alumina ratio of $SiO_2/Al_2O_3 = 3.0$. But the kaolin waste was calcined at 750 °C for 1 h, it was ground in ball mill for another 1 h, and its curing was carried out at 50 °C, differently from this work, where the kaolin was not calcined nor ground.

There is no research with the synthesis of geopolymeric cements using natural, non-processed kaolin. The references show works using metakaolin processed from natural kaolin by calcination and grounding, and modified synthesis conditions for the processed raw materials, and even so, the compressive strength for these works are not higher than that obtained in this work.

The results of this work are assigned to the amorphous nature and particle size of the natural kaolin used. These characteristics

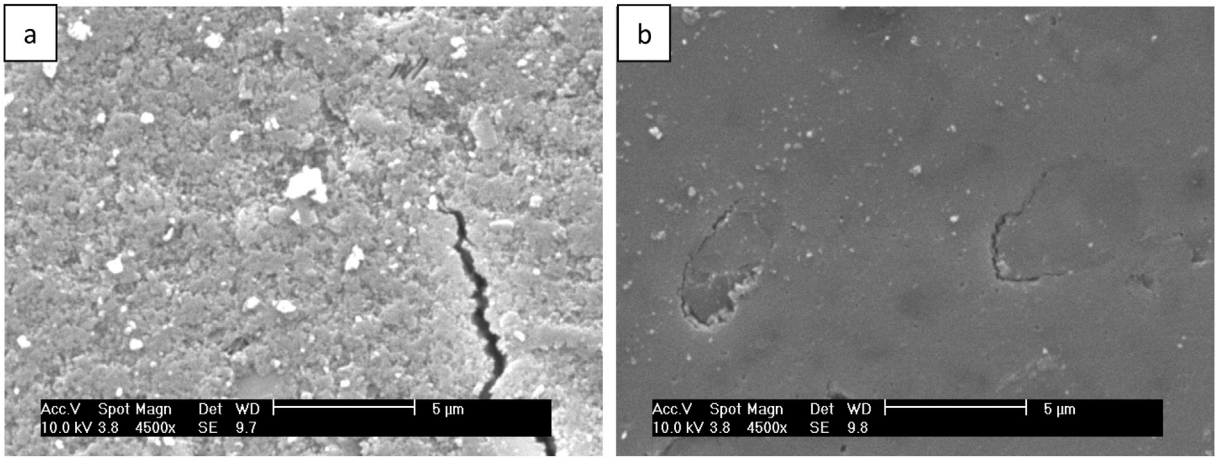

Fig. 8. SEM images of the surfaces of compositions: (a) K1, $Na_2O.SiO_2/NaOH = 2.2$; and (b) K3, $Na_2O.SiO_2/NaOH = 1.0$.

can be sought in other raw materials or industrial waste to produce geopolymeric cements, with the aim of reducing the environmental impact and the energy spent on the processing of the raw materials.

3.1. Reduction of environmental impacts by using natural kaolin in geopolymers

The kaolin used in this work is a regular raw material used by the ceramic industry to produce ceramic tiles, without any prior calcination. Therefore, the geopolymers produced in this work show less energy expenditure, lower cost and reduction in CO_2 emissions when compared to geopolymeric cements produced with metakaolin and mainly compared to Portland cement due to the use of a natural, non-calcined, kaolin. In addition to the reduction of CO_2 emissions, energy expenditure and cost, there is also the exclusion of the calcination step to obtain kaolin to be used as precursor for geopolymeric cements.

Also, as the geopolymers synthetized in this work were composed of approximately 50% natural kaolin and 50% sodium silicate and sodium hydroxide, the only environmental impacts are the CO_2 emissions and energy costs associated with the production of the alkaline precursors. However, some studies show that those costs and emissions are smaller than that of Portland cement (Van Deventer et al., 2012), therefore emphasizing the environmental advantage of using natural kaolin, even when comparing with the use of metakaolin as raw material for geopolymers.

Another reason for the synthesis and use of geopolymeric cements is their compressive strength after curing, which, in this work using natural kaolin, was approximately 65 MPa at 7 days of age. Several studies on geopolymeric cements show low strength after curing (<20 MPa), preventing their use for building and construction works. In this work, the compressive strength (65 MPa) is higher than that of Portland cement (ranging from 32 to 50 MPa at 28 days). The compressive strength of geopolymers based on metakaolin, developed by Pelisser et al. (2013), was very similar to this work due to the mineralogical characteristics of the kaolin used. Mortars (Pelisser et al., 2013) and concrete (Pelisser et al., 2018) prepared using geopolymeric cements based on metakaolin showed compressive strength of 55 MPa, for a standard cement to aggregates ratio (1 : 5 = cement: aggregates, by mass). These admixtures result in a sustainable and competitive consumption of cement (binder intensity) of approximately 7 kg $m^{-3} \cdot MPa^{-1}$.

Considering the above, the environmental and economic potential of using a cement composed with natural clay (plus sodium silicate and NaOH) gives the importance of geopolymeric cements in an industrial society where the reduction of CO_2 emissions and the mitigation of environmental impacts are fundamental for a safe and sustainable development.

4. Conclusions

In this work, a geopolymeric cement was produced using a natural amorphous kaolin. The kaolin was not calcined nor milled, and the derived geopolymeric cement can be considered a green cement. The geopolymeric cement showed high compressive strength, 65 MPa, due to an efficient polymerization process. The results of the micro-nanomechanical characterization showed a modulus of elasticity of 10.2 GPa and a hardness of 0.39 GPa for the composition $Na_2O.SiO_2/NaOH = 1.6$ (K2), results very close to the ones of the compositions K1 ($Na_2O.SiO_2/NaOH = 2.2$) and K3 ($Na_2O.SiO_2/NaOH = 1.0$).

The study shows that the degree of amorphism of the natural kaolin was determinant for the geopolymerization process and, in addition with the chemical composition, is the most important factor for the mechanical performance and the efficiency of the geopolymeric cements. These properties are important for the technological development of alternative cements and helps its application in the building industry.

Regarding the environmental impact and sustainability of geopolymeric cements produced from natural kaolin, the use of a non-calcined kaolin helps the reduction of costs and environmental impacts in the production of geopolymers, resulting in a green cement.

The synthesis of an alternative cement using natural, non-processed raw materials is of upmost importance to produce efficient cements to be used in the building industry, therefore reducing the environmental impacts, especially in countries with less resources. As the building industry is the largest economic activity in the world, considering resources and raw material consumption, the benefit of using an environmentally friendly (green) cement is evident.

Considering future work, the aim is to use the geopolymeric composition into concrete (adding aggregates) and measuring complementary properties as durability in aggressive environments (acids and sulfates), comparing the proposed geopolymeric cement to Portland cement. Also, using it in structural elements, evaluating the steel/concrete adhesion in improving the mechanical performance of concrete beams.

Funding

This work was funded by the Coordination for the Improvement of Higher Education Personnel of Brazil, National Council of Technological and Scientific Development of Brazil and the Foundation for Research Support and Innovation of the state of Santa Catarina, Brazil.

Data availability

Data will be available on request.

CRediT authorship contribution statement

Fernando Pelisser: Conceptualization, Methodology, Writing - review & editing. **Adriano Michael Bernardin:** Writing - original draft. **Milton Domingos Michel:** Methodology, Investigation. **Caroline Angulski da Luz:** Methodology, Investigation.

Declaration of competing interest

The authors declare that they have no known competing financial interests or personal relationships that could have appeared to influence the work reported in this paper.

Acknowledgements

The authors acknowledge the support of the Central Laboratory of Electronic Microscopy (LCME/UFSC, Brazil).

References

Amran, Y.H.M., Alyousef, R., Alabduljabbar, H., El-Zeadani, M., 2020. Clean production and properties of geopolymer concrete: a review. J. Clean. Prod. 251, 119679. https://doi.org/10.1016/j.jclepro.2019.119679.

Assi, L.N., Carter, K., Deaver, E., Ziehl, P., 2020. Review of availability of source materials for geopolymer/sustainable concrete. J. Clean. Prod. 263, 121477. https://doi.org/10.1016/j.jclepro.2020.121477.

ASTM C 1231, 2010. Standard Practice for Use of Unbonded Caps in Determination of Compressive Strength of Hardened Concrete Cylinders. ASTM International, West Conshohocken, PA, USA.

Bajpai, R., Choudhary, K., Srivastava, A., Sangwan, K.S., Singh, M., 2020. Environmental impact assessment of fly ash and silica fume based geopolymer concrete. J. Clean. Prod. 254, 120147. https://doi.org/10.1016/j.jclepro.2020.120147.

Brotzen, F.R., 1994. Mechanical testing of thin films. Int. Mater. Rev. 39, 24–44. https://doi.org/10.1179/imr.1994.39.1.24.

Cassagnabère, F., Mouret, M., Escadeillas, G., Broilliard, P., Bertrand, A., 2010. Metakaolin, a solution for the precast industry to limit the clinker content in concrete: mechanical aspects. Construct. Build. Mater. 24, 1109–1118.

Chindaprasirt, P., Chareerat, T., Sirivivatnanon, V., 2006. Workability and strength of coarse high calcium fly ash geopolymer. Cement Concr. Compos. 29, 224–229.

Davidovits, J., 1991. Geopolymers: inorganic polymeric new materials. J. Therm. Anal. 37, 1633–1656.

Firdous, R., Stephan, D., Djobo, J.N.Y., 2018. Natural pozzolan based geopolymers: a review on mechanical, microstructural and durability characteristics. Construct. Build. Mater. 190, 1251–1263. https://doi.org/10.1016/j.conbuildmat.2018.09.191.

Gartner, E., Sui, T., 2018. Alternative cement clinkers. Cement Concr. Res. 114, 27–39. https://doi.org/10.1016/j.cemconres.2017.02.002.

Heah, C.Y., Kamarudin, H., Mustafa, A.L., Bakri, A.M., Bnhussain, M., Luqman, M., Khairul-Nizar, I., Ruzaidi, C.M., Liew, Y.M., 2012. Study on solids-to-liquid and alkaline activator ratios on kaolin-based geopolymers. Construct. Build. Mater. 35, 912–922.

Longhi, M.A., Rodríguez, E.D., Bernal, S.A., Provis, J.L., Kirchheim, A.P., 2016. Valorisation of a kaolin mining waste for the production of geopolymers. J. Clean. Prod. 115, 265–272.

Ma, C.-K., Awang, A.Z., Omar, W., 2018. Structural and material performance of geopolymer concrete: a review. Construct. Build. Mater. 186, 90–102. https://doi.org/10.1016/j.conbuildmat.2018.07.111.

Medri, V., Papa, E., Lizion, J., Landi, E., 2020. Metakaolin-based geopolymer beads: production methods and characterization. J. Clean. Prod. 244, 118844. https://doi.org/10.1016/j.jclepro.2019.118844.

Nemecek, J., Smilauer, V., Kopecky, L., 2011. Nanoindentation characteristics of alkali-activated aluminosilicate materials. Cement Concr. Compos. 33, 163–170.

Ng, C., Alengaram, U.J., Wong, L.S., Moa, K.H., Jumaat, M.Z., Ramesh, S., 2018. A review on microstructural study and compressive strength of geopolymer mortar, paste and concrete. Construct. Build. Mater. 186, 550–576. https://doi.org/10.1016/j.conbuildmat.2018.07.075.

Oliver, W.C., Pharr, G.M., 1992. An improved technique for determining hardness and elastic modulus using load and displacement sensing indentation experiments. J. Mater. Res. 7, 1564–1583. https://doi.org/10.1557/JMR.1992.1564.

Oliver, W.C., Pharr, G.M., 2004. Measurement of hardness and elastic modulus by instrumented indentation: advances in understanding and refinements to methodology. J. Mater. Res. 19, 3–20. https://doi.org/10.1557/jmr.2004.19.1.3.

Ozel, M., 2012. Cost analysis for optimum thicknesses and environmental impacts of different insulation materials. Energy Build. 49, 552–559.

Palomo, A., Fernandez-Jimenez, A., Kovalchuk, G., Ordonez, L.M., Naranjo, M.C., 2007. OPC fly ash cementitious systems: study of gel binders produced during alkaline hydration. J. Mater. Sci. 42, 2958–2966.

Pelisser, F., Gleize, P.J.P., Michel, M.D., 2011. Nanomechanical properties of cement paste. Rev. IBRACON Estrut. Mater. 4, 561–574.

Pelisser, F., Gleize, P.J.P., Mikowski, A., 2012. Effect of the Ca/Si molar ratio on the micro-nanomechanical properties of synthetic C-S-H measured by nanoindentation. J. Phys. Chem. C 116, 17219–17227.

Pelisser, F., Guerrino, E.L., Menger, M., Michel, M.D., Labrincha, J.A., 2013. Micromechanical characterization of metakaolin-based geopolymers. Construct. Build. Mater. 49, 547–553.

Pelisser, F., Silva, B.V., Menger, M.H., Frasson, B.J., Keller, T.A., Torii, A.J., Lopez, R.H., 2018. Structural analysis of composite metakaolin-based geopolymer concrete. Rev. IBRACON Estrut. Mater. 11 (3), 535–543.

Provis, J., 2013. Geopolymers and other alkali activated materials: why, how, and what? Mater. Struct. 47, 11–25.

Provis, J.L., Palomo, A., Shi, C., 2015. Advances in understanding alkali-activated materials. Cement Concr. Res. 78, 110–125.

Rashad, A., 2013. Alkali-activated metakaolin: a short guide for civil Engineer. An overview. Construct. Build. Mater. 41, 751–765.

Reddy, M., Dinakar, P., Hanumantha, R., 2016. A review of the influence of source material's oxide composition on the compressive strength of geopolymer concrete. Microporous Mesoporous Mater. 234, 12–23.

Shia, C., Qua, B., Provis, J.L., 2019. Recent progress in low-carbon binders. Cement Concr. Res. 122, 227–250. https://doi.org/10.1016/j.cemconres.2019.05.009.

Singh, N.B., Middendorf, B., 2020. Geopolymers as an alternative to Portland cement: an overview. Construct. Build. Mater. 237, 117455. https://doi.org/10.1016/j.conbuildmat.2019.117455.

Sneddon, I.N., 1965. The relation between load and penetration in the axisymmetric boussinesq problem for a punch of arbitrary profile. Int. J. Eng. Sci. 3, 47–57. https://doi.org/10.1016/0020-7225(65)90019-4.

Tan, J., Cai, J., Li, X., Pan, J., Li, J., 2020. Development of eco-friendly geopolymers with ground mixed recycled aggregates and slag. Journal of Cleaner Production. J. Clean. Prod. 256, 120369. https://doi.org/10.1016/j.jclepro.2020.120369.

Turner, L.K., Collins, F.G., 2013. Carbon dioxide equivalent (CO_2-e) emissions: a comparison between geopolymer and OPC cement concrete. Construct. Build. Mater. 43, 125–130.

Van Deventer, J.S.J., Provis, J.L., Duxson, P., 2012. Technical and commercial progress in the adoption of geopolymer cement. Miner. Eng. 29, 89–104, 2012.

Zhang, P., Wang, K., Li, Q., Wang, J., Ling, Y., 2020. Fabrication and engineering properties of concretes based on geopolymers/alkali-activated binders: a review. J. Clean. Prod. 258, 120896. https://doi.org/10.1016/j.jclepro.2020.120896.